

## TEMPERATURE INDUCED CRYSTALLIZATION PROCESSES IN Nd<sub>2</sub>Fe<sub>14</sub>B/Fe<sub>3</sub>B MAGNETIC NANOCOMPOSITES

A.JIANU<sup>1</sup>, M.VALEANU<sup>1</sup>, D.P.LAZAR<sup>1</sup>, F.LIFEI<sup>1</sup>, M.TOMUT<sup>1</sup>, V.POP<sup>2</sup>,  
S.ALEXANDRU<sup>3</sup>

<sup>1</sup> National Institute for Materials Physics, P.O. Box Mg-7, 76900 Bucharest, Romania

<sup>2</sup> Faculty of Physics, Babes-Bolyai University, 3400 Cluj-Napoca, Romania

<sup>3</sup> S.C.ICPE-CA SA 74204, Bucharest, Romania

*Abstract.* The influence of Zr and Ti substitutions on the formation of a nanocomposite magnet was studied by high-temperature X-ray diffraction and magnetic measurements. It has been shown that Ti and especially Zr additions favorably change the crystallization temperatures and the sequence of phase transformations which leads to an exchange coupled magnet, even in a composition range that promotes the precipitation of the detrimental Nd<sub>2</sub>Fe<sub>23</sub>B<sub>3</sub> phase.

*Key words:* Nd-Fe-B nanocomposites; Crystallization processes; Metastable phases .

Short title max 60 lit: Hard Magnetic Nanocomposites

The exchange spring phenomena are related to the pinning of a soft magnetic (SM) phase by a hard magnetic (HM) phase, via exchange interactions, which act at the interface between the two phases in contact. The system has excellent hard magnetic properties: the hard magnetic phase give rise to a high anisotropy and coercivity whereas the soft magnetic phase enhances the saturation magnetization. Due to their unusual high remanence, large energy product and low cost, the exchange spring magnets provided attractive potential applications as permanent magnets. Micromagnetic calculations [1] and experimental results have shown that the exchange coupling is achieved in nanocomposite materials in which the hard magnetic (RE<sub>2</sub>Fe<sub>14</sub>B) and the additional soft ( $\alpha$ -Fe or Fe<sub>3</sub>B) nanophases, are crystallographic coherent.

Nanocomposite exchange spring magnets may be obtained from amorphous ribbons with RE-Fe-B defined composition, using suitable annealing treatments. By reducing the rare-earth content the crystallization process becomes more complex due to the formation of some metastable phases, most of them magnetic soft; the decomposition of these phases requires high temperatures or long heat treatment which leads to crystallites coarsening. In nanocomposite Nd<sub>2</sub>Fe<sub>14</sub>B/Fe<sub>3</sub>B or  $\alpha$ -Fe the magnetic properties are strongly

related to the microstructure. The optimum structure consists of uniformly distributed soft and hard magnetic nanophases. In practice, it is difficult to control the grain size; microalloying elements (e.g. Cu, Nb, Ga, W, and Si [2, 3]) have been used in many cases to optimize the microstructure. The present work deals with a study of the microalloying effects of Zr and Ti substitution on the evolution of crystallization process and the magnetic hardening of the  $\text{Nd}_7\text{Fe}_{81}\text{B}_{12}$  alloy.

## 1. EXPERIMENTAL

Ingots with nominal compositions  $\text{Nd}_7\text{Fe}_{81}\text{B}_{12}$ ,  $\text{Nd}_7\text{Fe}_{81}\text{Ti}_2\text{B}_{10}$  and  $\text{Nd}_7\text{Fe}_{79}\text{Zr}_2\text{B}_{12}$  were prepared by arc melting. Amorphous ribbons (25 $\mu\text{m}$  thickness) were obtained by melt spinning in argon atmosphere. The temperature-induced crystallization processes were studied *in situ* using synchrotron radiation in high-temperature energy-dispersive x-ray diffraction experiments (HASY-LAB, F2.1 beam line). Phase composition and magnetic behavior were analyzed on samples heated for 2-5 minutes, in vacuum, at temperatures between 650 and 800 $^{\circ}\text{C}$ . Conventional XRD measurements were performed using Cu  $\text{K}\alpha$  radiation. Hysteresis loops were obtained by the extraction method at room temperature, in fields up to 1.8 T, applied along the length of the ribbons.

## 2. RESULTS AND DISCUSSIONS

High-temperature energy-dispersive x-ray diffraction (EDXRD) using synchrotron radiation was performed for the evaluation of phase transformations process. Fig.1 shows the diffraction patterns of the free substitution sample (the temperature range 300 - 850 $^{\circ}\text{C}$ ); even at the highest temperature,  $\text{Nd}_2\text{Fe}_{23}\text{B}_3$  was detected as a predominant phase. It is to note that the Nd fluorescence lines at 36.84, 37.36, 42.27 and 43.32 KeV are superposed on the diffraction spectra. The crystallization process starts at 600 $^{\circ}\text{C}$  with the precipitation of the  $\text{Nd}_2\text{Fe}_{23}\text{B}_3$  metastable phases. The first diffraction peaks of the  $\text{Nd}_2\text{Fe}_{14}\text{B}$  phase become visible at 700 $^{\circ}\text{C}$ . The selected composition has the stoichiometry near that of the  $\text{Nd}_2\text{Fe}_{23}\text{B}_3$  phase. A missing composition gradient around metastable phase grains induces a low rate of atomic diffusion. This may explain the high value of the decomposition temperature.

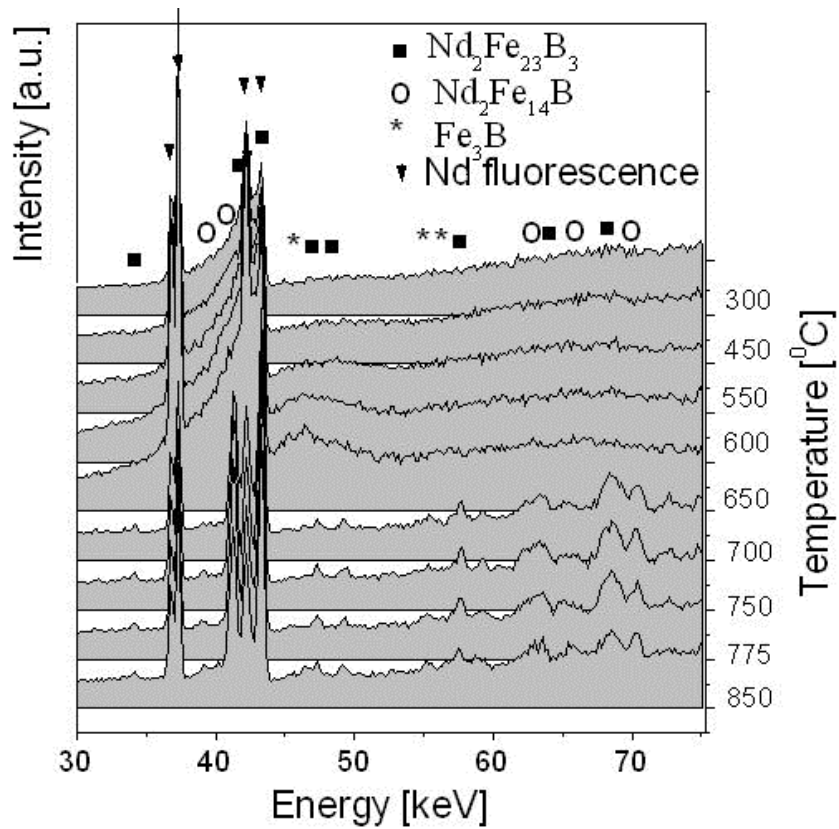


Fig.1

*In situ* high temperature EDXRD measurements of rapidly solidified Nd<sub>7</sub>Fe<sub>81</sub>B<sub>12</sub>.

For the Nd<sub>7</sub>Fe<sub>81</sub>Ti<sub>2</sub>B<sub>10</sub> sample, the crystallization also starts at 600 °C with the formation of Nd<sub>2</sub>Fe<sub>23</sub>B<sub>3</sub>, but this phase decomposes into Fe<sub>3</sub>B and Nd<sub>2</sub>Fe<sub>14</sub>B at 650 °C. The X-ray diffraction patterns for these samples, after 5 minutes of heat treatment at 650 °C and 700 °C, illustrate this decomposition (Fig 2a and 2b, respectively).

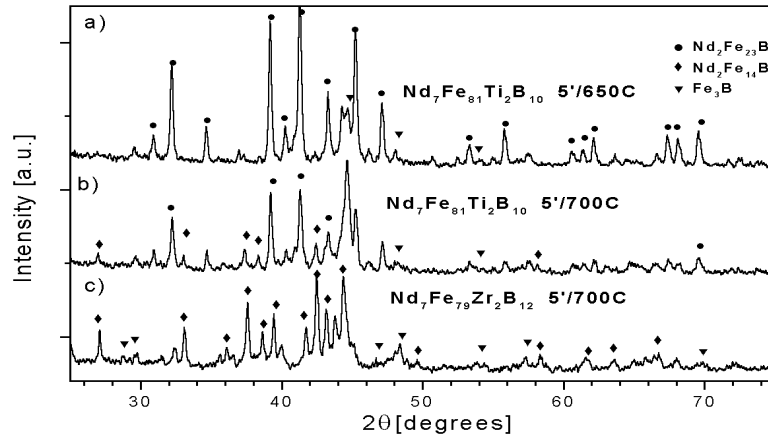


Fig. 2

X-Ray diffraction patterns for  $\text{Nd}_7\text{Fe}_{81}\text{Ti}_2\text{B}_{10}$  (a and b) and  $\text{Nd}_7\text{Fe}_{79}\text{Zr}_2\text{B}_{12}$  (c) alloys after different annealing treatments

This behavior is confirmed by the thermomagnetic measurements performed on a sample annealed at 650°C for 5 minutes and presented in Fig.3. During heating, the metastable phase  $\text{Nd}_2\text{Fe}_{23}\text{B}_3$ , is still present, but after reaching  $\sim 800^\circ\text{C}$ , the cooling curve shows that  $\text{Nd}_2\text{Fe}_{23}\text{B}_3$  has fully decomposed.

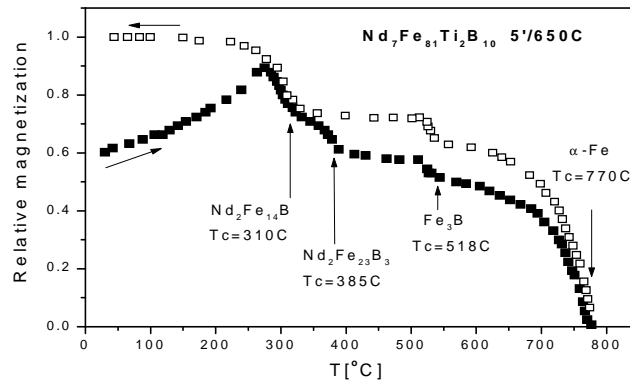


Fig. 3

Thermomagnetic measurements performed on  $\text{Nd}_7\text{Fe}_{81}\text{Ti}_2\text{B}_{10}$  sample annealed at 650°C for 5 minutes

For the sample with Zr substitution, the crystallization process is different:  $\text{Nd}_2\text{Fe}_{14}\text{B}$  and  $\text{Fe}_3\text{B}$  precipitate directly from the amorphous phase. This behavior confirms the influence of Zr atoms in stabilizing the 2:14:1 phase [2].

The exchange coupling between the soft and hard phases was checked by magnetic measurements on annealed samples. For  $\text{Nd}_7\text{Fe}_{81}\text{B}_{12}$  and  $\text{Nd}_7\text{Fe}_{81}\text{Ti}_2\text{B}_{10}$ , the saturation magnetization decreases with increasing the annealing temperature, suggesting the decomposition of  $\text{Nd}_2\text{Fe}_{23}\text{B}_3$ . The high temperature crystallization of the hard magnetic phase in  $\text{Nd}_7\text{Fe}_{81}\text{B}_{12}$  allows the grain growth of the  $\text{Fe}_3\text{B}$  phase, which becomes too large for an exchange coupling. Fig. 3 presents the hysteresis loop of  $\text{Nd}_7\text{Fe}_{81}\text{B}_{12}$  with the highest coercivity obtained after a heat treatment of 5 minute at  $775^\circ\text{C}$ ; it shows a typical behavior of a hard/soft mixture without exchange coupling.

Ti substitution for boron has a beneficial effect on the exchange coupling, by reducing the  $\text{Nd}_2\text{Fe}_{23}\text{B}_3$  decomposition temperature; after annealing for 2 min. at  $725^\circ\text{C}$  (Fig. 4), the remanence ratio  $M_r/M_s$  of 0.71 indicates the existence of intergranular exchange interactions. Nevertheless the shoulder in the demagnetization curve shows an imperfect coupling between the magnetic phases, the size of the soft one been probably too large.

The best magnetic exchange coupling is obtained for  $\text{Nd}_7\text{Fe}_{79}\text{Zr}_2\text{B}_{12}$ . An optimum coercivity of 3.7kOe, a remanence ratio of 0.81 (Fig. 4) and an energy product of 10.9GOe are obtained on a sample annealed for 2 minutes at  $700^\circ\text{C}$ .

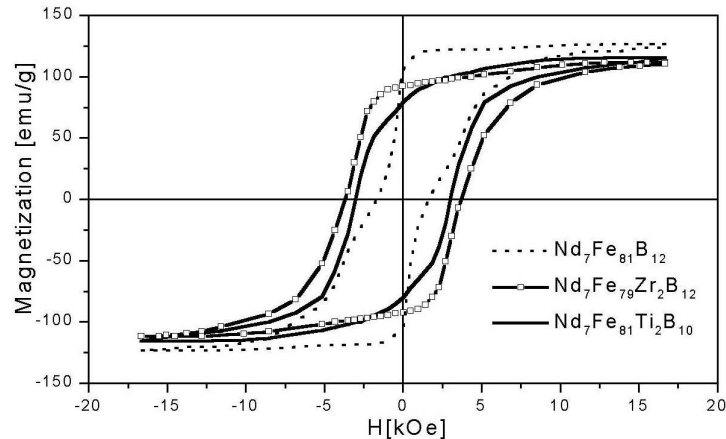


Fig. 4

Room-temperature hysteresis loops after the optimized annealing treatments

### 3. CONCLUSION

The selected composition –  $\text{Nd}_7\text{Fe}_{81}\text{B}_{12}$  – has the stoichiometry near that of the  $\text{Nd}_2\text{Fe}_{23}\text{B}_3$  phase. The precipitation of a  $\text{Nd}_2\text{Fe}_{14}\text{B}/\text{Fe}_3\text{B}$  mixture takes place by the decomposition of the metastable, primarily formed  $\text{Nd}_2\text{Fe}_{23}\text{B}_3$  phase. A lack of composition gradient around metastable phase grains induces a low rate of atomic diffusion during annealing. The high value of the decomposition temperature induces a final non-uniform microstructure, unsuitable for an exchange coupled magnet.

2% Ti substitution for B reduced the decomposition temperature preserving some exchange coupling.

2% of Fe atoms substituted by Zr changed the sequence of the crystallization process promoting the formation of  $\text{Nd}_2\text{Fe}_{14}\text{B}/\text{Fe}_3\text{B}$  nanocomposite in the first step, at lower temperatures and the improvement of the magnetic properties.

#### Acknowledgement

Work partial supported by the Institute of Atomic Physics under CERES Program, Grant 11/C1.2001

#### Reference

- [1] E.F.KNELLER, R.HAWING, IEEE Trans.Mag. 27, 358, 1991
- [2] D.H.PING ET AL., Acta Mater, 47, 4641, 1999
- [3] D.H.PING ET AL. J.Mag.Mag.Mat., 239, 437, 2002